Supporting Information

Polyphenol-Enhanced Extreme-Environment Adaptive Hydrogels for High-Altitude Burn Wound Repair

Shengxi Jiang ‡[a, b], Yujia Zheng ‡[a, b], Peiji Yang [a], Huabin Liu [a], Wei Zhang [b], Yanan Jiang [c], Liwei Yan [d], Jie Weng [a, b], Feng Lin [e, *], Hongyu Sun [f, *], Xiong Lu [a, b, *], Chaoming Xie [a, b, *]

a Institute of Biomedical Engineering, College of Medicine, Southwest Jiaotong University, Chengdu 610031, Sichuan, China.

b Key Lab of Advanced Technologies of Materials, Ministry of Education, School of Materials Science and Engineering, Southwest Jiaotong University, Chengdu, Sichuan, 610031, China.

c Obesity and Metabolism Medicine-Engineering Integration Laboratory, Department of General Surgery, Medical Research Center, Affiliated Hospital of Southwest Jiaotong University, The Third People's Hospital of Chengdu, Chengdu, China.

d Sports Medicine Center, Department of Orthopedic Surgery/Orthopedic Research Institute, West China Hospital, Sichuan University, Chengdu, Sichuan 610064, China.

e Department of Thoracic Surgery, West China Hospital, Sichuan University, Chengdu, Sichuan 610064, China.

f Center for Animal Experimentation, Clinical Biobank, and Bioinformatics, The General Hospital of Western Theater Command, Chengdu, 610083, China.

*Corresponding author(s). E-mail(s): xie@swjtu.edu.cn (Chaoming Xie); luxiong_2004@163.com (Xiong Lu); sunhongyu@swjtu.edu.cn (Hongyu Sun); linfeng0220@yeah.net (Feng Lin)

‡ These authors contributed equally to this work.

1. Materials

Gelatin from porcine skin was purchased from Sigma. Gallic acid, branched chain starch, ammonium persulfate, sodium hydroxide, anhydrous calcium chloride, 1,2-dimethylimidazole were purchased from Aladdin. Hydrogen peroxide, ammonia, zinc nitrate, and methanol were purchased from Chengdu Cologne. Other chemical reagents were all purchased from Mecolin, China.

2. Experimental methods

2.1 Preparation of oxygen-releasing ZIF-8

Dissolve 10 g of $CaCl_2$ in 50 mL of deionized water, and then add it to a beaker containing 600 mL of anhydrous ethanol. Stir vigorously for 10 minutes. Next, add 50 mL of a 30% (mass fraction) H_2O_2 solution and continue stirring for 2 minutes. Slowly add 50 mL of ammonia at a concentration of 1 mol/L, and stir vigorously for 30 minutes. Perform centrifugal washing with anhydrous ethanol twice. After washing, freeze-dry the mixture to obtain CaO_2 powder.

Next, dissolve 4.5 g of Zn $(NO_3)_2$ in 20 mL of methanol. Dissolve 10 g of dimethylimidazole in another 20 mL of methanol. Disperse 1 g of CaO_2 nanoparticles in the methanol solution of dimethylimidazole using stirring and ultrasonic treatment for 10 minutes. Pour the Zn $(NO_3)_2$

solution into the above system, mixing and stirring for 10 hours. Finally, centrifuge the mixture and wash it with anhydrous ethanol three times to obtain ZIF-8@CaO_2 oxygen-releasing ZIF-8.

2.2 Preparation of hydrogels

Firstly, 0.2 g of gallic acid (GA) was dissolved in 8.8 mL of deionized water to form a GA solution at 60 °C. Then, 1.2 mL of NaOH solution (concentration of 5 g/10 mL) was added, and GA was oxidized and polymerized to PGA after a reaction time of 30 minutes. Next, 1 g of Gel and 1 g of AP were dissolved in 8 mL of the solution at 95 °C, and the mixture was stirred for 20 minutes until the starch was completely pasted. To the Gel-AP solution, 1 mL of PGA solution was added at 95 °C with stirring for 3 minutes. Then, 1 mL of deionized water was added to disperse 0.2 g of ZIF-8@CaO_2, which were then incorporated into the system while stirring at 95 °C for 5 minutes to form a Gel-AP-PGA- ZIF-8@CaO_2 (GAPN) solution. To this GAPN solution, 200 μL of a 0.2 g/mL ammonium persulfate solution was added at 95 °C with stirring for 10 seconds, and then the mixture was poured into a polytetrafluoroethylene plate mold to form a gel and obtain the GAPN hydrogel.

3 Characterization

3.1 Scanning electron microscopy analysis of oxygen-releasing ZIF-8

The surface morphology of ZIF-8@CaO_2 was observed using a scanning electron microscope (SEM, JSM 6390, JEOL, Japan) equipped with X-ray energy dispersive spectroscopy (EDS).

3.2 Transmission electron microscopy analysis of oxygen-releasing ZIF-8

The morphological structure of ZIF-8@CaO_2 nanoparticles was studied using transmission electron microscopy (TEM, JSM 2100F, JEOL, Japan). The elemental distribution of ZIF-8@CaO_2 was analyzed by energy dispersive X-ray spectroscopy (EDS).

3.3 X-ray diffraction analysis of oxygen-releasing ZIF-8

X-ray diffraction spectra of ZIF-8@CaO_2 were obtained using an X-ray diffractometer (Rigaku Ultima IVX, Rigaku, Japan) operating at 40 kV and 40 mA. CuKα filtered irradiation (λ = 1.5406 nm) was utilized. Before testing, the ZIF-8@CaO_2 nanoparticle dispersion was freeze-

dried to obtain dry ZIF-8@CaO_2 nanoparticles.

3.4 Oxygen release performance analysis of oxygen releasing ZIF-8

0.2 g of ZIF-8@CaO_2 nanoparticles and 0.05 g of CaO_2 nanoparticles were each dispersed in 10 mL of PBS. The amount of dissolved oxygen was measured at regular intervals using a dissolved oxygen meter (JB608, Remagnet, Shanghai, China). At the end of each measurement, the samples were centrifuged and re-dispersed by adding an equal volume of PBS. The dissolved oxygen value of the real-time PBS was subtracted from the dissolved oxygen value of each measurement to determine the amount of oxygen produced by the nanoparticles during that time period. Measurements were taken from day 1 to day 7. A cumulative release curve of the oxygen produced by the nanoparticles over time was generated.

3.5 Analysis of the free radical generating properties of oxygen-releasing ZIF-8

10 mg of ZIF-8@CaO_2 was dispersed in 0.5 mL of phosphate buffer at pH 6 and pH 7.4, respectively. After 30 minutes, the supernatants were centrifuged and added to 2.5 mL of acetate buffer. Subsequently, 100 μL of 3,3‘,5,5’-tetramethylbenzidine (TMB) at a concentration of 10 mg/mL was added, and the mixture was incubated for 30 minutes at room temperature. The free radical content was then determined at 652 nm using a UV-vis spectrometer (TU-1901, Puxi, China).

3.6 Mechanical properties of hydrogels

(1) Tensile test

Tensile tests were performed using a universal testing machine (UTM, Instron 5567, USA) at a loading rate of 2 mm/min. Hydrogels with a thickness of 2 mm were cut into strips measuring 25 mm in length and 25 mm in width. The distance between the clamps was set at 5 mm. Tensile force (F) was divided by the cross-sectional area (A) to obtain the tensile stress (σ), calculated as $\sigma = F/A$. The tensile strain (ε) was determined by dividing the difference between the length after stretching (L) and the original length (L_0) by L_0, expressed as $\varepsilon = (L - L_0)/L_0$.

(2) Compression test

The compression test was conducted using a universal testing machine (UTM, Instron 5567) with a 100 N load cell and a loading speed of 5 mm/min. The hydrogel samples had dimensions of 10 mm in height and 10 mm in diameter. The compressive force (F) was divided by the cross-sectional area (A) to obtain the compressive stress (σ), calculated as $\sigma = F/A$. The compressive strain (ε) was determined by dividing the difference between the height before compression (H_0) and the height after compression (H) by H_0, expressed as $\varepsilon = (H_0 - H)/H_0$.

(3) Cyclic tensile and compression tests

In cyclic tensile experiments, GAPN hydrogels were first stretched to a maximum tensile strain of 100% at a crosshead speed of 2 mm/min, followed by a relaxation period for recovery. In cyclic compression tests, the specimens were initially compressed to a fixed strain of 50% at a crosshead speed of 5 mm/min, then allowed to relax for recovery. A total of 10 cycles were performed for both tests.

(4) Adhesion Test

The tissue adhesion strength of different hydrogels was measured using an adhesion-tension test. Fresh pig skin served as the typical tissue. Briefly, the hydrogel was applied to the pig skin over a bonding area of 20 mm × 20 mm and pre-pressurized with 15 N for 10 seconds. The samples were then pulled using a universal testing machine (UTM, Instron 5567) equipped with a load of 100 N at a crosshead speed of 2 mm/min until separation occurred. The bond strength was calculated by dividing the maximum load by the initial bonding area. The bond strength of GAPN hydrogels was also tested against hydrophilic glass, hydrophobic polytetrafluoroethylene (PTFE), and metallic materials (titanium sheets) using the same method.

3.7. Testing of hydrogels for UV resistance

Transmission and UV absorption spectra of the hydrogels in the range of 200–800 nm were measured using a UV-Vis spectrophotometer (TU-1901) equipped with hydrogen and tungsten lamps. The hydrogel sample had dimensions of 30 mm × 10 mm × 2 mm. The hydrogel was applied to the back of suckling mice, and after 5 minutes of UV light irradiation, skin samples

from both the hydrogel-covered and uncovered areas were collected for H&E staining.

3.8. Anti-freezing test of hydrogels

Different hydrogels containing 60% glycerol were prepared and stored at -40 °C for 24 hours to observe their state. The phase transition point (freezing point) of various hydrogels without glycerol was determined using differential scanning calorimetry (DSC). GAPN hydrogels with 60% glycerol were shaped to dimensions of 1 cm × 2 mm × 5 cm, stored at -40 °C for 24 hours, and then subjected to tensile testing.

3.9 Density functional theory (DFT) study

To investigate the interactions between the components of the hydrogel formed by glycerol and water, Density Functional Theory (DFT) calculations were employed to analyze these intermolecular forces. All DFT calculations were conducted using the Dmol3 module in the Materials Studio software suite (Accelrys, San Diego, CA). This software represents the wave functions of the simulated system through numerical basis sets, enabling Dmol3 to provide high computational accuracy while optimizing efficiency. For these calculations, we used the DNP (3.5) numerical basis set, recognized for its robustness in modeling molecular interactions. To approximate the exchange-correlation energy, we applied the Perdew-Burke-Ernzerhof (PBE) functional within the Generalized Gradient Approximation (GGA) framework. The geometrical optimization and single-point energy calculations adhered to the following convergence criteria: (1) The convergence criterion for the self-consistent field calculation was set at 1.0×10^{-6} Ha/atom. (2) The energy convergence criterion was set at 1.0×10^{-5} Ha/atom. (3) The maximum stress error was limited to 0.002 Ha/Å. (4) The maximum displacement error was limited to 0.005 Å.

(1) Model building

Prepolymerized gallic acid and water (PGA-water model), prepolymerized gallic acid and glycerol (PGA-glycerol model), prepolymerized gallic acid and water/glycerol (PGA-water-glycerol model).

(2) Interaction Energy Calculations

The interaction energy (E_{int}) expresses the strength of the interaction between the components of the system. It is derived from the following equation:

$$E_{int} = E_{total} - \sum E_{component} \quad \text{(Equation S1)}$$

Where E_{total} and $E_{component}$ represent the total energy of the system, and the energy of each component in the system, respectively.

3.10 Oxygen release properties of hydrogels

After 10 mL of the hydrogel precursor solution was formed into a gel in a mold, it was placed in a sample bottle containing 20 mL of phosphate buffer. The oxygen content was measured at regular intervals using a dissolved oxygen meter. At the end of each test, the liquid was poured off, and an equal volume of phosphate buffer was added. The dissolved oxygen value measured at each time point was subtracted from the dissolved oxygen value of the real-time phosphate buffer to determine the amount of oxygen produced by the hydrogel during that period. Measurements were taken separately for 1 to 7 days, and a cumulative release curve of oxygen produced by the hydrogel over time was generated.

3.11 Antioxidant property test of hydrogel

First, a DPPH solution with a concentration of 40 μg/mL was prepared. Then, 3 mL of the DPPH solution was added to hydrogels with a diameter of 10 mm and a thickness of 2 mm, and the samples were placed in the dark at 37 °C. Pure DPPH solution was used as a control. After a predetermined time, the supernatant was collected following high-speed centrifugation, and the absorbance of the DPPH solution was measured at 517 nm using a TU-1901 UV-visible spectrophotometer, with methanol solution serving as the blank baseline. The formula for calculating DPPH radical scavenging efficiency is as follows:

$$DPPH\ scavenging\ (\%) = \frac{A_B - A_S}{A_B} \times 100\% \quad \text{(Equation S2)}$$

A_B represents the absorbance of DPPH solution; A_S represents the absorbance of DPPH solution after reaction with the sample.

3.12 Ion release property testing of hydrogels

6 g of GAPN hydrogels were placed in equal amounts of phosphate buffer at pH 6 and pH 7.4, respectively, and then incubated in a 37 °C environment. The supernatant was collected at various time intervals, and the concentration of elemental Zn in the solution was determined using atomic absorption spectroscopy, while the concentration of elemental Ca was measured using a calcium content detection kit.

3.13 In vitro antimicrobial testing of hydrogels

In vitro antimicrobial activity assays were performed using Staphylococcus epidermidis (S. epidermidis, ATCC 6538, a gram-positive organism) and Escherichia coli (E. coli, ATCC 8739, a gram-negative organism) to evaluate the antimicrobial properties of different hydrogels. A 50 μL aliquot of bacterial suspension (1 × 10^6 CFU/mL) was added to the samples. After 4 hours, 1 mL of Luria-Bertani broth medium was added, and the samples were placed in an incubator at 37 °C. After 12 hours, 20 μL of the bacterial suspension was taken for plating, and 100 μL of the suspension was used to measure its absorbance (OD) at 600 nm using an enzyme marker (MQX200). The antibacterial rate of each group was calculated using the following formula:

$$Antibacterial\ rate\ (\%) = \frac{OD_{control} - OD_{sample}}{OD_{control}} \times 100\% \qquad \text{(Equation S3)}$$

The different hydrogels were co-cultured with the biofilms for 12h, then they were stained live/dead and the biofilm status was observed using laser confocal microscopy.

3.14 Cell activity assay in hypoxic environment

Different hydrogel samples were used for cell activity testing in a low oxygen environment. The dimensions of the hydrogel samples were 8 mm in diameter and 1 mm in thickness. Before cell inoculation, the samples were sterilized with 75% ethanol and then purified with sterile PBS and culture medium to remove residual ethanol. Then, 2×10^4 individual umbilical vein

endothelial cells were inoculated into 24-well plates and cultured for 4 h for wall apposition before adding hydrogel. 1m L of culture medium was added to each well. The 24-well plates were placed in a low oxygen chamber containing 1% oxygen at 37° C. Cells were grown adherent to the wall for 1 and 3 days, and the biocompatibility and cell proliferation of the hydrogels were examined using live/dead staining assay and Cell Proliferation and Activity Assay Kit (CCK-8). The morphology of the cells was observed with a laser scanning confocal microscope (CLSM, LSM880, Carl Zeiss, Germany).

3.15 Cell migration assay in hypoxic environment

Human umbilical vein endothelial cells were inoculated into 24-well plates with 5×10^4 cells per well, and the cell layer was scraped off with a pipette tip when the cell concentration reached approximately 90%. Subsequently, different hydrogels were implanted, and the cell migration rate was quantified after being placed into a low oxygen environment with an oxygen content of 1% for 24h.

3.16 Expression of cellular hypoxia-inducible factors in hypoxic environments

RAW264.7 macrophages were inoculated in 24-well plates with 3×10^5 added to different hydrogels per well and analyzed by HIF-1α immunofluorescence staining after co-culturing for 24h in an environment with 1% oxygen.

3.17 In vitro reactive oxygen species scavenging experiments with hydrogels

In vitro scavenging of ROS was performed with different hydrogels, respectively. The size of the hydrogels was Φ15 mm × 2 mm. first, 3.0 × 105 RAW 264.7 cells were inoculated in each well of a 24-well plate. 300 μL of culture medium was added to each well. Then the 24-well plate was placed in a humidified incubator at 37° C with 5% CO2. After 4 h of incubation, 500 μL of 50 μM hydrogen peroxide per well was added for stimulation.After 12 h, the hydrogel and medium were removed, and the cells were washed with PBS for 3 times. 500 μL

of 2', 7' dichlorodiacetic acid dichlorofluorescein (S0033, Biyoungtian) was added to each well. After incubation in the dark for 20 min, cells were washed 3 times with PBS. Cell morphology was observed with a laser confocal microscope (LSM880, Carl Zeiss). Blank wells without hydrogen peroxide treatment were used as negative control, and blank wells treated with hydrogen peroxide were used as positive control.

3.18 In vitro anti-inflammatory activity of the hydrogel

RAW264.7 macrophages were seeded into 6-well plates at a density of 5×10^6 cells per well, with 1 mL of culture medium added to each well. Once the cells adhered to the well surfaces, 1 μg of lipopolysaccharide (LPS) was added to stimulate them, followed by the addition of hydrogel. The cells were then co-cultured for 24 hours under hypoxic conditions (1% O_2). After incubation, the medium and hydrogel were removed. The cells were subsequently immunofluorescence stained for CD86 and CD206 markers, respectively. Cell morphology and fluorescence were observed using laser scanning confocal microscopy, and the relative fluorescence intensity was quantitatively analyzed.

3.19 In vivo biological evaluation of hydrogels

To further investigate the performance of the hydrogel in promoting burn wound healing in plateau and plain environments, we constructed a burn wound model using healthy SD rats (male, weighing 300-350 g, Chengdu Dashuo). The experiments were conducted in accordance with the protocol approved by the Ethics Committee and the regulations on laboratory animal management in China. The animal ethics approval number is SWJTU-2403-NSFC (076), which was granted by the relevant institutional review board.

Establishment of burn model: (1) After anesthetizing the rats with 3% sodium pentobarbital (0.2 mL/100 g), their backs were shaved and further depilated using depilatory cream. Any residual hair and cream were washed off with saline, followed by disinfection of the depilated area using iodophor and 75% alcohol in succession. (2) A heated metal rod (100 °C, diameter 1.5 cm) was applied to the surface of the bare back in a vertical position for 20 seconds to create a full-thickness skin burn. The necrotic tissue at the burn site was then removed with

medical scissors to establish a full-layer skin burn defect with a circular wound measuring 2 cm in diameter. (3) A 50 μL suspension (1 × 10^6 CFU/mL) containing a mixture of Escherichia coli and Staphylococcus epidermidis was added dropwise to each wound. (4) Four groups were established: the untreated group (Blank), the Gel-AP group, the Gel-AP-PGA group, and the GAPN group, with the corresponding materials implanted. The wounds were covered with Tegaderm™ dressings and placed into the respective environments after the rats were awakened from anesthesia.

(1) Skin repair for burn infections

Plains burn infection was modeled using the steps outlined above (1-4) and the rats were placed in plains environment for rearing. At one day postoperatively, the plain burn infection model was assessed by taking wound tissue and incubating it in Luria-Bertani broth medium for 24 hours. Photographs were taken at 0, 5, 10, 15, and 23 days postoperatively to document the healing process. The rats were euthanized at 5 and 23 days postoperatively, respectively, and both the wound site and surrounding tissues were collected. These samples were fixed in 4% paraformaldehyde solution, embedded in paraffin wax, and sliced into thin sections of 5 μm thickness. Sections from 5 days postoperatively were subjected to immunofluorescence staining for CD86 and CD206 to evaluate the level of inflammation at the wound. Sections from 23 days postoperatively were assessed using various techniques: H&E staining to evaluate the repair effect of the hydrogel on burn wounds, Masson staining to analyze collagen deposition, and immunofluorescence staining for PGP9.5, CK14, CD31, and α-SMA to assess nerve repair, neoepidermal maturation, and angiogenesis resulting from the hydrogel treatment in different environments.

(2) Skin repair for burns in the high-altitudes

The above steps (1, 2, 4) were conducted in an environmental simulation chamber maintained at an altitude of 5000 m (an atmospheric pressure of 54 kPa, oxygen partial pressure of 11kPa and a temperature of 25°C) to establish a plateau burn model. The plateau burn model was photographed at 0, 5, 10, 15, and 23 days post-surgery to document the healing process. The rats were euthanized at 5 and 23 days postoperatively, and both the wounds and surrounding

tissues were collected, fixed in 4% paraformaldehyde solution, embedded in paraffin wax, and sliced into thin sections of 5 μm thickness. Sections from 5 days postoperatively were assessed for levels of hypoxia, inflammation, and angiogenesis at the wound site using immunofluorescence staining for HIF-α, HSP70, HO-1, CD86, CD206, CD31, and α-SMA. Sections from 23 days post-surgery were evaluated using H&E immunohistochemistry to assess the hydrogel's repair effect on burn wounds, Masson staining to evaluate collagen deposition, and immunofluorescence staining for PGP9.5 and CK14 to assess nerve repair and neoepidermal maturation of the hydrogel treatment in different environments.

3.20 Statistics and analyses

All experiments were repeated more than three times, and the results are presented as mean ± standard deviation. p-values were generated using one-way analysis of variance (ANOVA) followed by Tukey's multiple comparisons post hoc test, with $n \geq 3$. Significance thresholds were defined as follows: * ($p < 0.05$), ** ($p < 0.01$), and *** ($p < 0.001$).

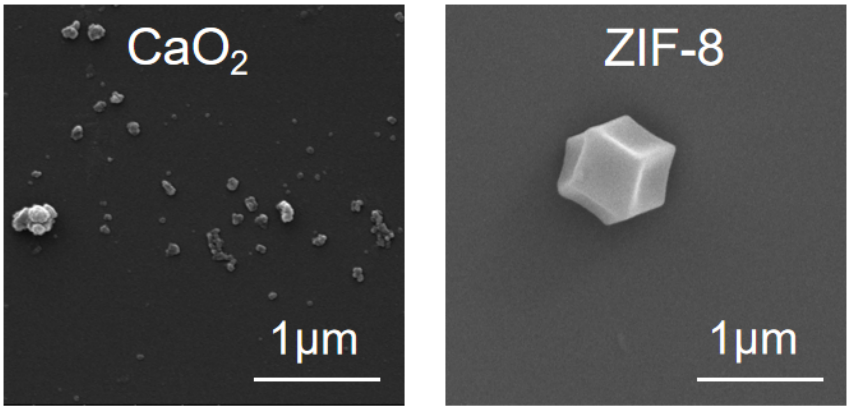

Figure S1. SEM images of CaO_2 and ZIF-8.

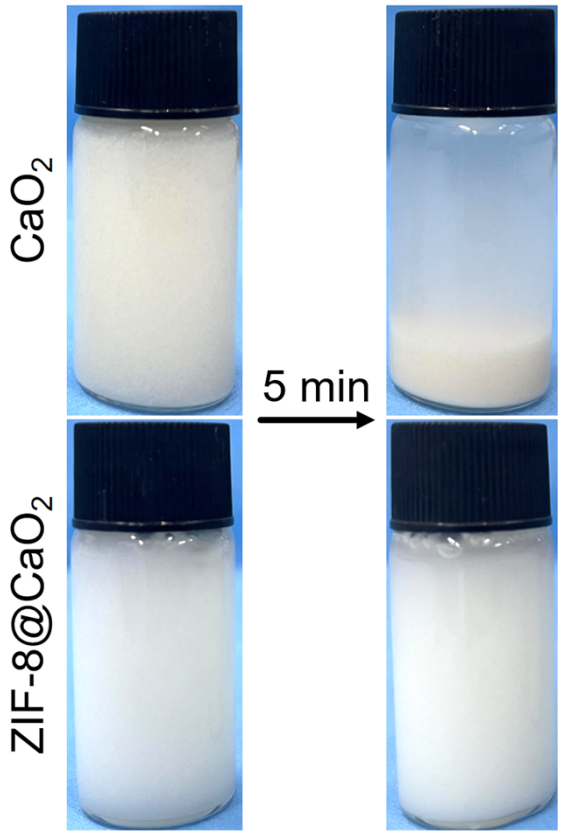

Figure S2. Photographs of CaO_2 and ZIF-8@CaO_2 dispersions in water solution.

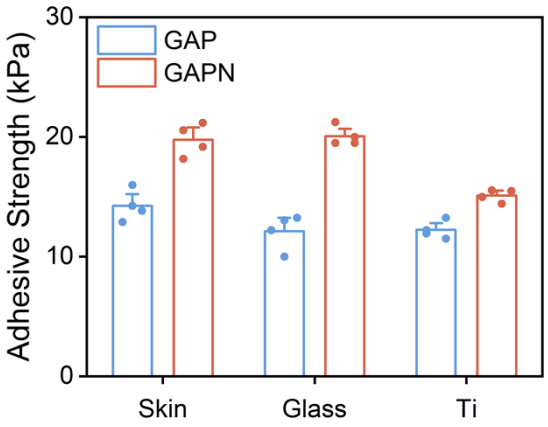

Figure S3. Adhesion strength of hydrogels to different substrates.

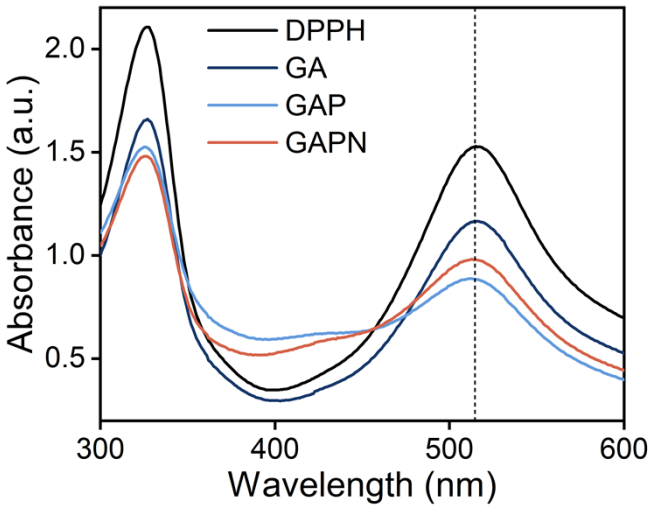

Figure S4. UV-visible absorption spectra of different hydrogels after reacting with DPPH free radicals for 50 minutes.

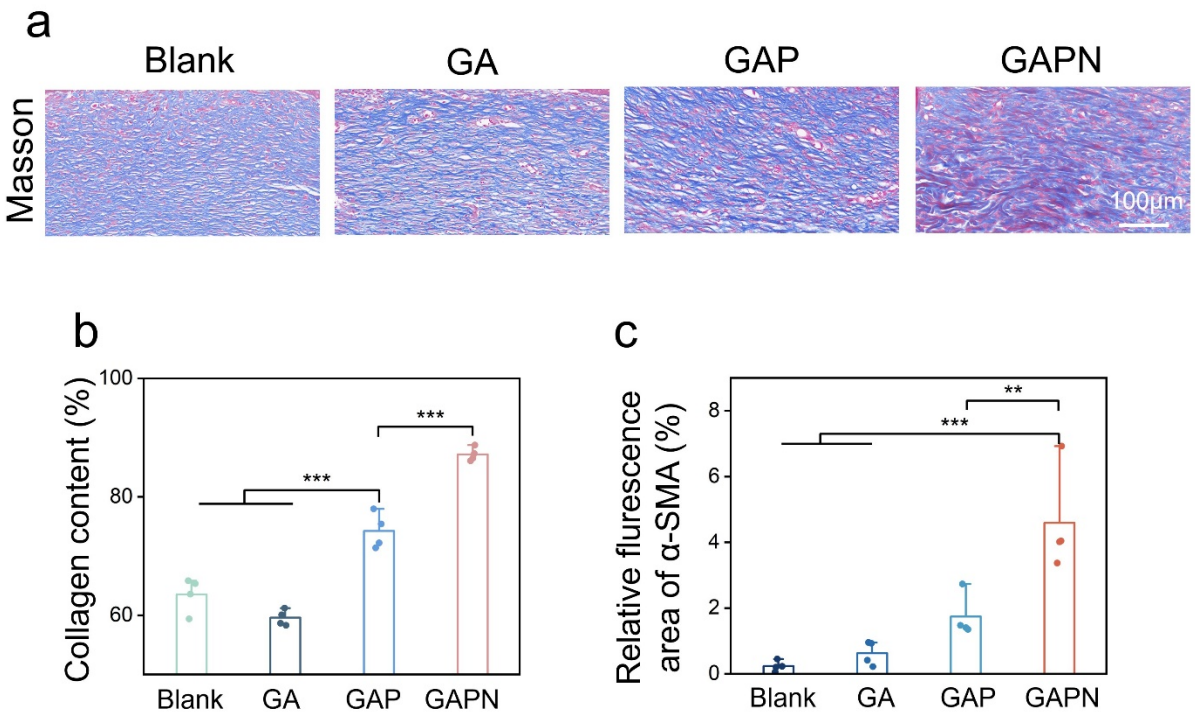

Figure S5. (a) Masson staining of burn wounds in different hydrogel treatment groups after 23 days. (b) Quantitative analysis of the collagen deposition level in the wound. (c) Relative fluorescence area quantitative analysis of α-SMA.

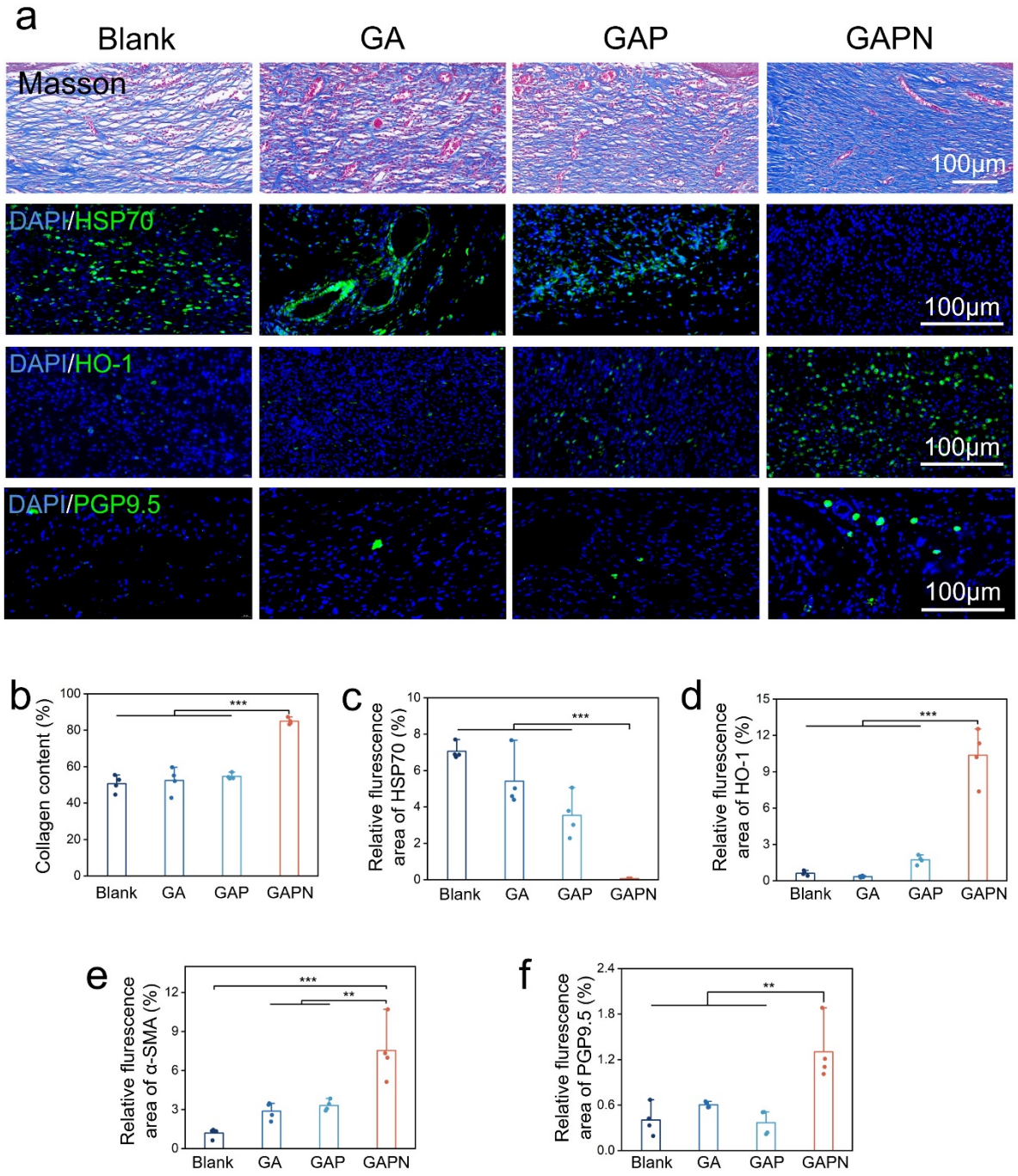

Figure S6. (a) Masson staining of burn wounds in different hydrogel treatment groups after 23 days; Immunofluorescence staining images of HSP70 and HO-1 of burn wound tissue after 5days, and PGP9.5 after 23days. (b) Quantitative analysis of the collagen deposition level in the wound. Relative fluorescence area quantitative analysis of (c) HSP70, (d) HO-1, (e) α-SMA, (f) PGP9.5.

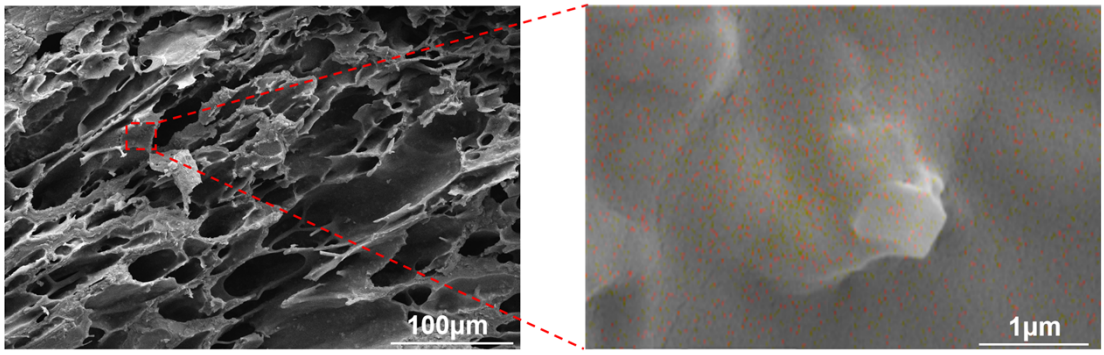

Figure S7. Scanning electron microscopy characterisation of GAPN hydrogels.

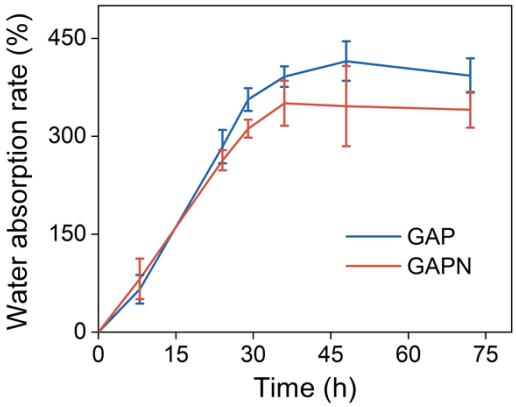

Figure S8. Water absorption ratio curve of GAP and GAPN hydrogels.

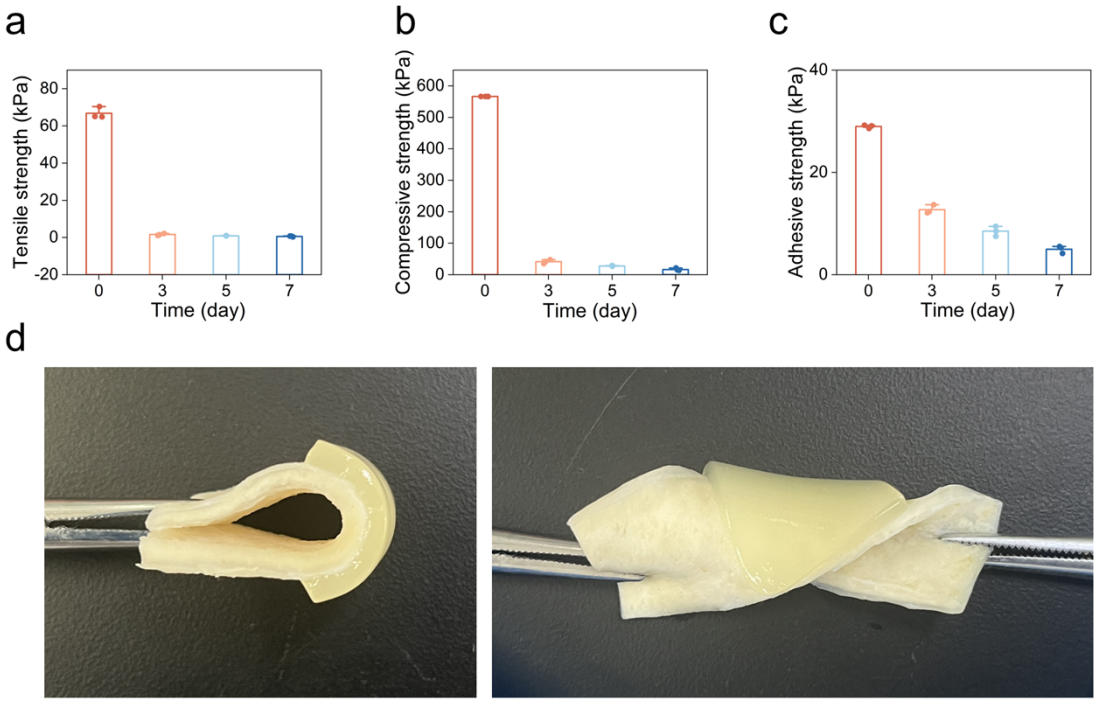

Figure S9. (a) Tensile strength; (b) Compressive strength; (c) Adhesion strength of GAPN hydrogel over time in PBS at 37°C. (d) Photograph of hydrogel adhesion behavior on pig skin after 7 days in PBS at 37°C.

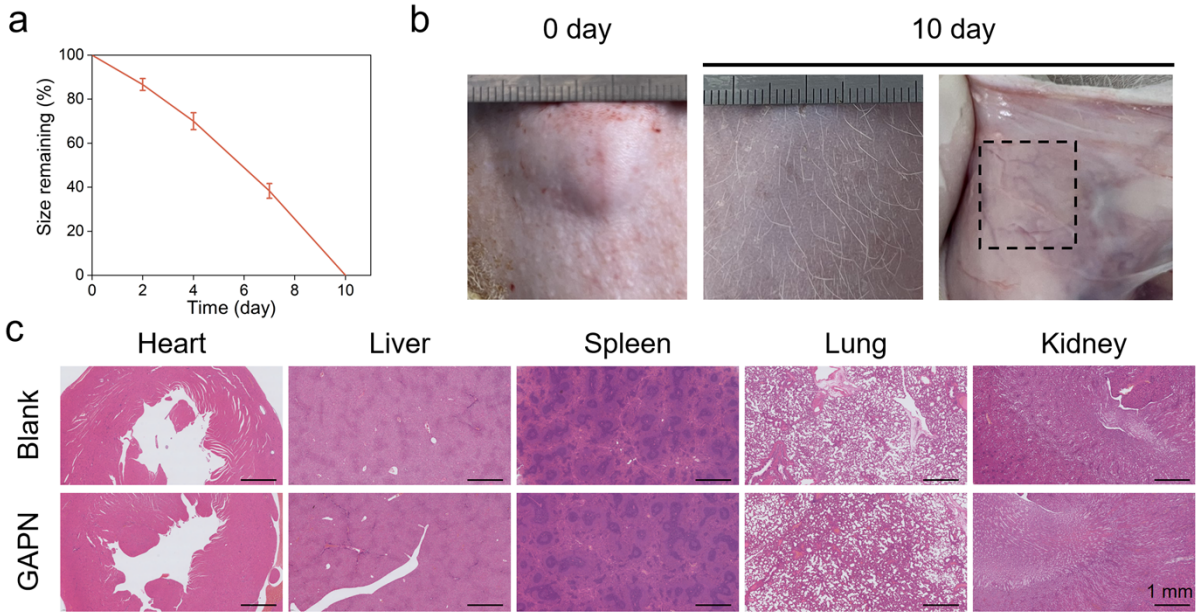

Figure S10. (a) In vivo degradation curve of GAPN hydrogels. (b) Photographs of GAPN hydrogel in vivo degradation at 0 days and 10 days. (c) H&E staining images of heart, liver, spleen, lung, and kidney from normal rats and rats implanted with GAPN hydrogel after 10 days.

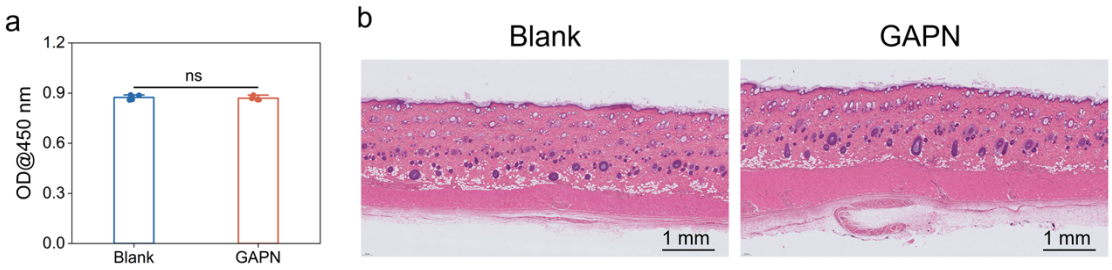

Figure S11. (a) Cell viability assessed by CCK-8 assay. (b) H&E staining images of rats 10 days after subcutaneous implantation of GAPN hydrogel.

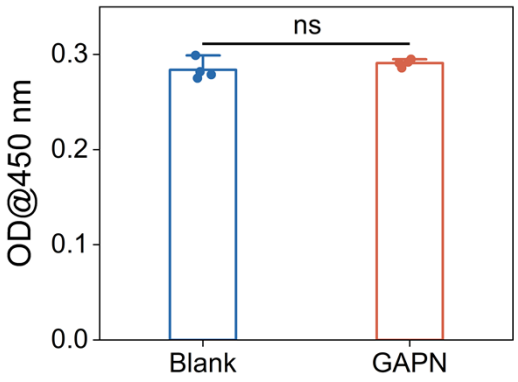

Figure S12. Following one day of co-culture of L929 cells with GAPN hydrogel in a pH 6 environment, cell viability was assessed using the CCK-8 assay.